

155
100406
19980621

SAND 97-3094 C
SAND-97-3094C
CONF-980218--

RECEIVED

MAR 09 1998

OSTI

Sandia hypervelocity gun technology for
validating EOS at extreme pressures and temperatures

Lalit C. Chhabildas, Michael D. Furnish, Rebecca M. Brannon, William D. Reinhart

Sandia National Laboratories, Shock Physics Applications, Department 9575, P. O. Box 5800,
Albuquerque, New Mexico 87185-1181, USA*

At very high impact velocities material properties will be dominated by phase-changes, such as melting or vaporization. These phase changes are not easily attainable at typical light-gas gun velocities of 8km/s. Development of well-controlled shock loading capabilities is the first step necessary to improve our understanding of material behavior at extreme pressures and temperatures not currently available using conventional two-stage light-gas gun techniques. In this paper, techniques that have been used to extend both the launch capabilities of a two-stage light gas gun to 16 km/s, and their use to determine the material properties at pressures and temperature states higher than those ever obtained using two-stage light-gas gun loading techniques are summarized. The newly developed hypervelocity launcher (HVL) can launch intact (macroscopic dimensions) plates to 16 km/s. Time-resolved interferometric techniques have been used to determine shock-loading/release characteristics of aluminum impacted by an aluminum flier, and shock-induced vaporization phenomena in fully vaporized zinc at impact velocities of 10 km/s. These experiments also define the maximum stress limit *i.e.*, 200 GPa to which lithium-fluoride windows can be utilized as a laser velocity interferometer window.

1. INTRODUCTION

Until approximately six years ago, two-stage light-gas guns [1-3] produced the highest pressure and temperature states in material that can be achieved in the laboratory using impact loading techniques. This generally involves performing impact studies at impact velocities of 8 km/s using high impedance impactor materials such as tantalum or platinum. A suite of diagnostic and experimental techniques [4,5] are then used to measure material properties in the high-pressure, high-temperature shocked state induced in materials at these impact velocities. These techniques allow measurements of the shock-Hugoniot [6], shock-loading and release behavior [7,8], material strength [6-10], shock-induced melting [8, 11-12], and shock-induced vaporization [11-12] processes in materials. The measurement of these material properties forms a data base to develop constitutive models to represent material behavior in dynamic loading [13].

There is a need to determine the equations of state of materials in regimes of extreme high pressures, temperatures and strain rates that are not attainable on current two-stage light-gas

* Sandia is a multiprogram laboratory operated by Sandia Corporation, a Lockheed Martin Company for the US Department of Energy under contract DE-AC04-94AL85000.

DISCLAIMER

This report was prepared as an account of work sponsored by an agency of the United States Government. Neither the United States Government nor any agency thereof, nor any of their employees, makes any warranty, express or implied, or assumes any legal liability or responsibility for the accuracy, completeness, or usefulness of any information, apparatus, product, or process disclosed, or represents that its use would not infringe privately owned rights. Reference herein to any specific commercial product, process, or service by trade name, trademark, manufacturer, or otherwise does not necessarily constitute or imply its endorsement, recommendation, or favoring by the United States Government or any agency thereof. The views and opinions of authors expressed herein do not necessarily state or reflect those of the United States Government or any agency thereof.

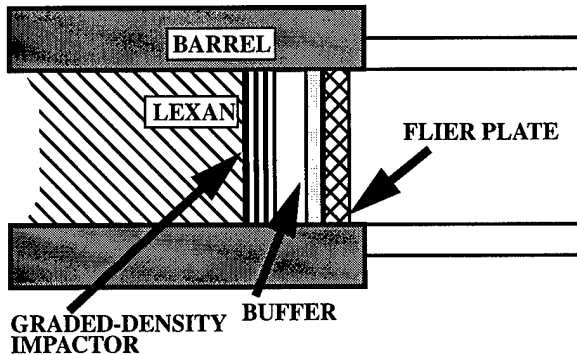


Figure 1(a). The Hypervelocity Launcher (HVL). Configuration used to launch flier plates to hypervelocities.

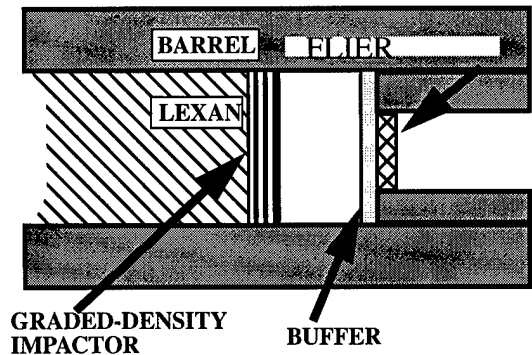


Figure 1(b). Enhanced HyperVelocity Launcher, (EHVL). Configuration used to launch confined flier plates in a tungsten barrel to hypervelocities.

described in Figure 1(b) to allow the launching of titanium and aluminum plates to velocities approaching 16 km/s [16]. The experimental design shown in Figure 1(b) acts as a dynamic acceleration reservoir which further enhances the flier plate velocity [16]. This is the highest mass-velocity capability attained with laboratory launchers to date, and therefore should open up investigations into new regimes of impact physics using various diagnostic tools [4,5].

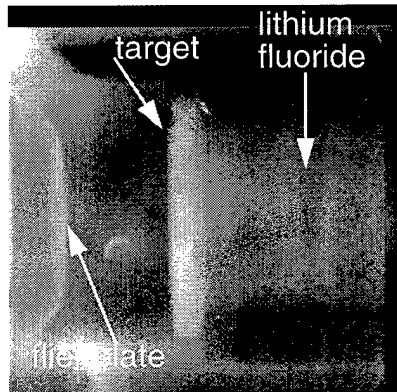


Figure 2(a). Radiograph of a titanium flier plate (prior to impacting a titanium target). The flier-plate is traversing at 9.60 km/s

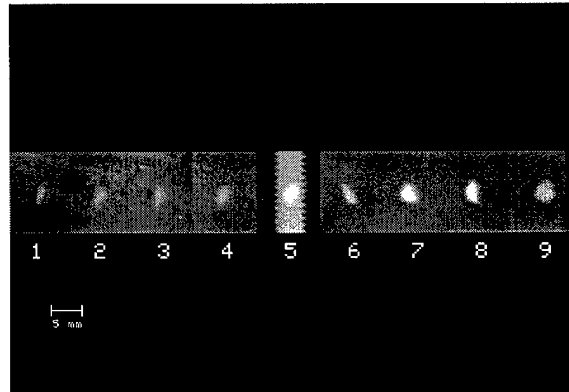


Figure 2(b). Radiographs of a titanium flier-plate traversing from left to right at a speed of 14.4 km/s over a flight distance of 1400 mm.

Due to the severe loading conditions which result from time-dependent megabar loading pressures, the flier plate achieves peak velocities over tens of millimeter acceleration distances. The plate appears to be "flat" for approximately the first thirty millimeter flight distances (see Figure 2(a)), and will then generally "bow" with increasing flight path. Flier plates have been launched intact and radiographed to flight distances of 1.4 meters from launch as indicated in Figure 2(b). Even though shockless loading conditions are used to accelerate the flier plate, the final temperature of the flier plate upon acceleration is approximately 600 K for the geometry used in Figure 1(a) after achieving velocities of 10 km/s. This is "cold" compared to its melt

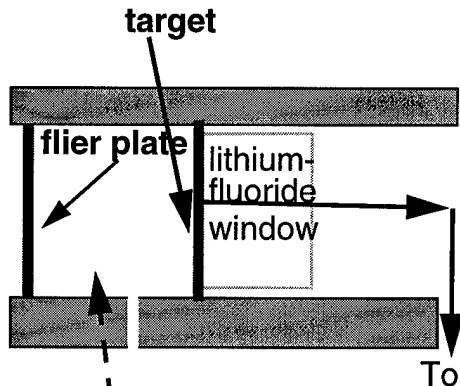


Figure 3(a). HVL configuration for shock-loading and release experiments. Resultant loading and release is measured as particle-velocity history at the target lithium-fluoride window interface.

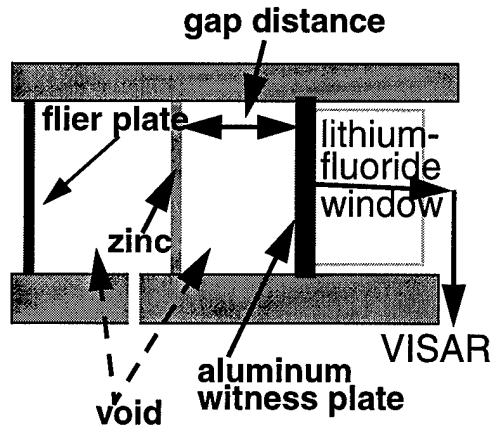


Figure 3(b). HVL configuration for vaporization experiments. The stagnation velocity history resulting from vaporized zinc is measured at the target lithium-fluoride window interface.

temperature, despite using enormous energy (compared to its melt and vaporization energy) to achieve hypervelocities. Designs using lower-impedance buffers such as foam can further reduce the temperature of the accelerating flier-plate.

3. EXPERIMENTAL CONFIGURATIONS

We have used the hypervelocity launcher (HVL) to perform one-dimensional plate-impact experiments. To achieve one-dimensional conditions, the target plate is stationed ~ 20 mm from the flier-plate. This ensures that the flier plate achieves peak particle velocity prior to impact, and remains relatively flat (see Figs. 2(a) & 5(a)) prior to impact. No attempt has been made to date to characterize the *planarity* of the impacting flier plate. The experimental configuration used to perform shock-loading and release measurements and shock-induced vaporization experiments are shown in Figure 3(a) and 3(b), respectively.

3.1 Shock-Loading and Release Experiments

The experimental configuration used to determine the shock loading and release states is described in Figure 3(a). Symmetric plate-impact experiments have been performed using aluminum, titanium, and tantalum at impact velocities of ~ 10 km/s. Figure 2(a) shows the radiograph of an experiment in which a 0.56 mm titanium alloy (Ti-6Al-4V) flier-plate is launched at 9.6 km/s prior to impacting a 2.0 mm thick titanium alloy target. The lithium-fluoride window[19] is clearly seen in the radiograph in Figure 2(a). The flat portion of the flier-plate prior to impact as observed in the radiograph is 19 mm. Note that for the full duration of the experiments there is a void behind the flier-plate; this allows measurements of a complete release from the shocked state. As indicated in Figure 3(a), a velocity interferometer VISAR [20], is used to estimate the particle-velocity history at the sample/lithium-fluoride window interface. The time-resolved particle velocity history measurements at the target/lithium-fluoride window interface are shown in Figure 4(a) and 4(b) for aluminum and titanium, respectively. Since no fiducial was established in these experiments, the shock arrival time at the target/window-

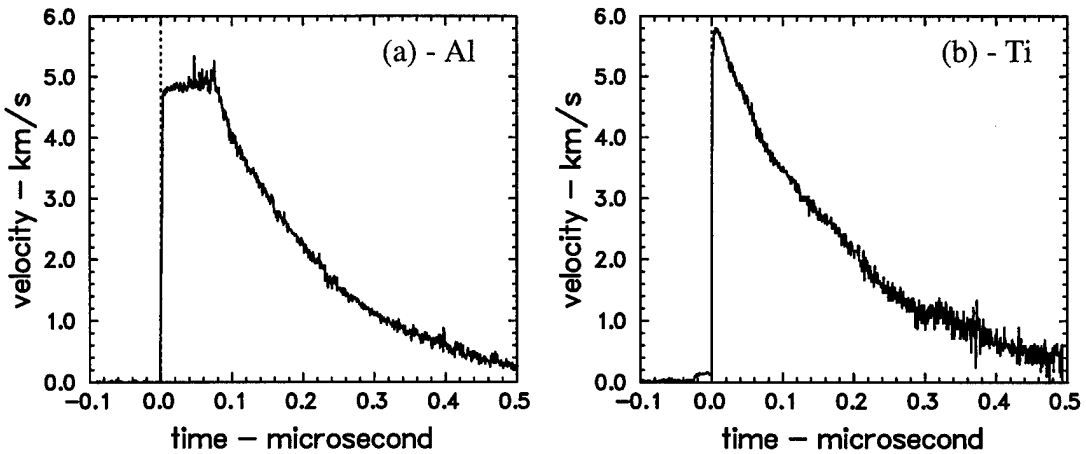


Figure 4. Measured interface particle velocity history for shock-loading and release experiments in (a) 6061-T6 aluminum at an impact velocity of 9.95 km/s, and (b) Ti-6Al-4V alloy at an impact velocity of 9.6 km/s. Symmetric impact configuration was used in both experiments.

interface is arbitrarily set to zero.

Figure 4(a) depicts the shock loading and release profile in aluminum shocked to 1.62 Mbar at an impact velocity of 9.95 km/s. In this experiment, a 0.98 mm thick aluminum flier-plate impacts a 1.98 mm thick aluminum target. Notice that a sustained shock of approximately 80 ns is observed in the figure prior to release. The titanium alloy is shocked to 2.3 Mbar at an impact velocity of 9.6 km/s, and a complete release profile as indicated in Figure 4(b) is measured. A profile resembling wave attenuation is measured in the titanium experiment because a thin flier plate (0.56 mm) impacts a thick (2.0 mm) target. Both experiments indicate a lack of elastic-plastic release structures—a clear indication of complete melt. These release structures then determine the off-Hugoniot states of materials shocked to extremely high-pressure

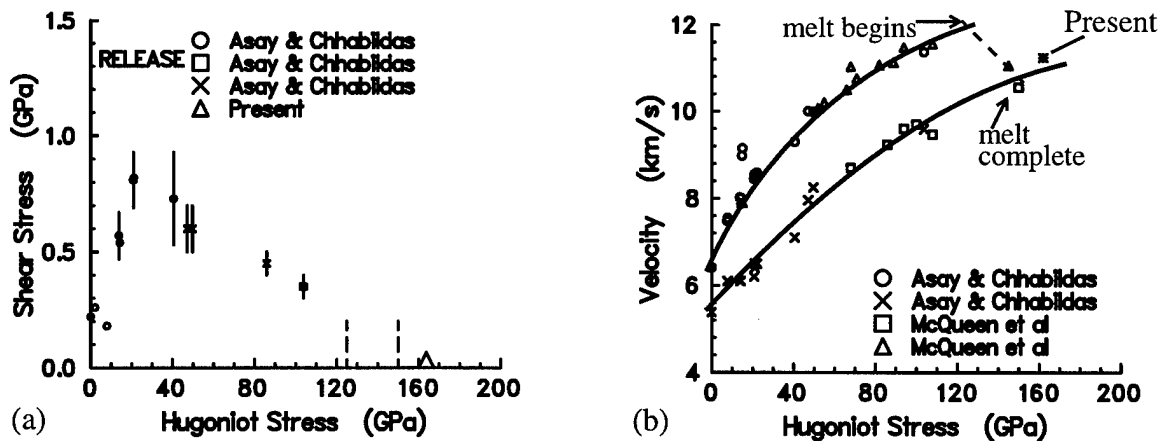


Figure 5. Measurements of (a) shear stress and (b) sound speed at 162 GPa in aluminum as determined from the release wave profile indicated in Figure 4 (a). Comparison with previous studies by Asay and Chhabildas [7,8] and McQueen et al [22] is also indicated.

Aluminum Experiment: The lack of elastic-plastic release clearly indicates complete melt in the shocked state at 1.62 Mbar. The shock Hugoniot state is based on measurements of the impact velocity and the existing equation of state for aluminum [21] given by the shock-velocity(U_s)-particle (u_p) velocity relation as ($U_s = 5.386 \text{ (km/s)} + 1.339 u_p$). The leading edge of the release wave velocity i.e the sound speed in the shocked state at 1.62 Mbar can be calculated knowing the sample and impactor dimensions, the dwell time of the shock at the sample-window interface, and the impact velocity. The calculated value of 11.24 km/s agrees very well with extrapolation of previous sound speed measurements by Asay and Chhabildas [7,8] and McQueen *et al* [22]. and is shown in Figure 4.

Lithium-Fluoride Window Transparency: The successful measurements reported in Figure 4, demonstrate the transparency of the lithium-fluoride (LiF) window at much higher pressures (and temperatures) than this window material has ever been subjected to before [19], *i.e.*, to 1.6 Mbar and 2 Mbar, respectively, in the aluminum and titanium experiment. Previous study has demonstrated transparency of LiF windows to stresses of 1.2 Mbar [19]. A symmetric impact experiment at 8.62 km/s using both tantalum as a target and as a flier plate, however, did not yield a release profile measurement similar to those in Figure 4. This corresponds to a stress of ~ 6.4 Mbar in tantalum and ~ 2.4 Mbar in the LiF window. This pressure level causes an apparent transparency loss in the LiF window. This is indicated in Figure 6. The beam intensity monitor (not shown) suggests that at 1.6Mbar stress level there is no loss of transparency, yielding extremely good fringe data at the sample-LiF window interface. As the stress level is increased to 2Mbar in the window there is considerable decrease in the in the beam intensity signal (See fig.6) but nevertheless reasonable fringe information is determined at the sample window interface. At a stress level of 2.4 Mbar in the window material there is a substantial decrease in the beam intensity signal and a total loss of fringe information from the sample/window interface; there is a total loss of contrast suggesting a reflection of the shock front. In short, the window interferometry technique using lithium fluoride windows is restricted for use up to shock stresses of 2Mbar in the window material. These results also point to the need to develop new time-resolved techniques and/or new window materials to allow successful measurements of off-Hugoniot states at extremely high pressures.

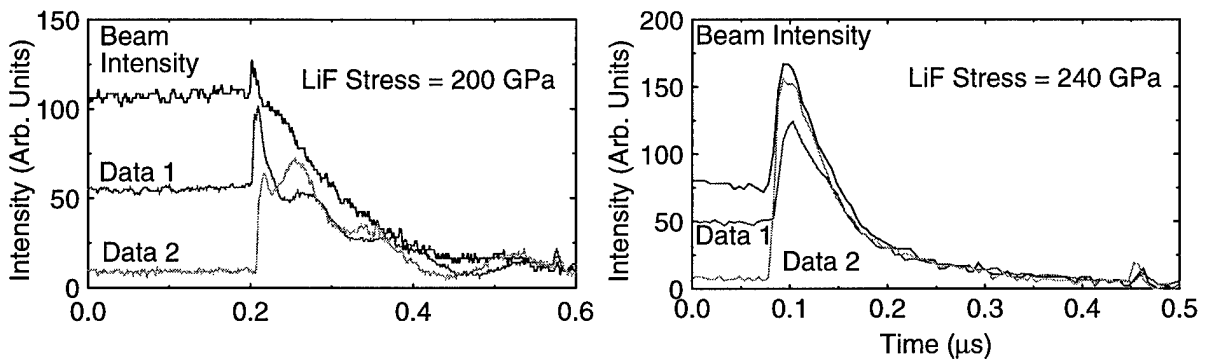


Figure 6. VISAR interferometer signals from sample/lithium-fluoride window interface suggesting a total loss of beam intensity, fringe data and contrast when the LiF is shocked to 240GPa. The use of lithium-fluoride window as an interferometric window is limited up to a shock stress of ~ 200 GPa , (left) at which stress fringe informatuon is still available.

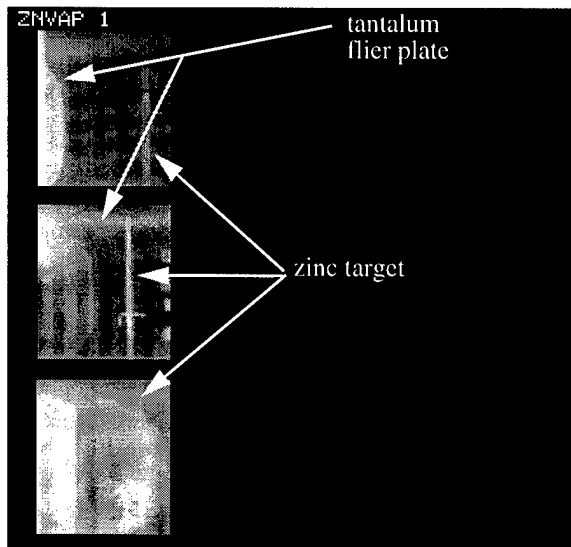


Figure 7(a). Radiographs of a tantalum flyer plate launched to velocities of 10.1 km/s prior to impacting a zinc target in the final frame using HVL.

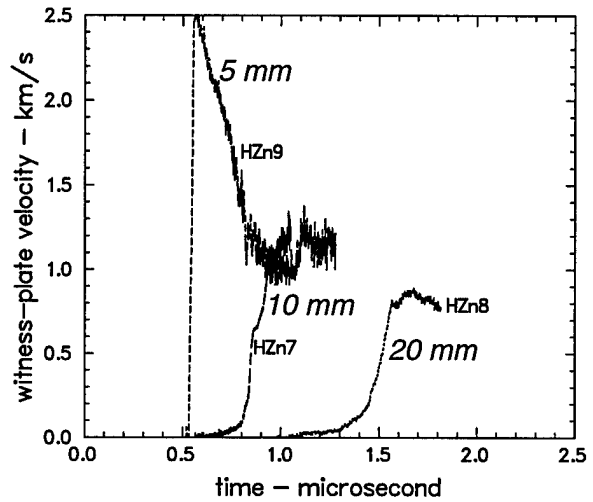


Figure 7(b). Measured stagnation particle velocity histories of shock-induced vaporization experiments conducted at an impact velocity of 10.1 km/s.

3.2 Shock-Induced Vaporization Experiments

This section briefly describes the use of the hypervelocity launcher to probe the kinetics of the shock-induced vaporization process in materials [17]. These results represent the first time-resolved measurements of *full vaporization* in zinc [17] resulting from release from stress states over the range of 3 Mbar to 5.5 Mbar, and temperatures as high as 39,000 K (3.4eV) in the zinc target [17]. (The release isentrope computed from a shock pressure of 5.5 Mbar and 39,000 K pass near the zinc critical point and it is therefore believed that full vaporization of zinc target occurs.) The experimental schematic is indicated in Figure 3(b), while the radiographs of the experiment are depicted in Figure 7(a). Following the arrival of the compressive wave at the free surface of the zinc target, a decompression wave propagates back into the zinc sample, which is now in a mixed phase of liquid and vapor. The rarefied liquid-vapor products left in the wake of this wave traverse a gap of known dimensions and stagnate against an aluminum witness plate backed by a lithium-fluoride laser-interferometer window [19]. The stagnation velocity history is determined through the use of a velocity interferometer [20], VISAR. Measured time-resolved stagnation particle velocity histories of experiments conducted at an impact velocity of 10.1 km/s are shown in Figure 5(b). In these experiments [17] the vaporized products are allowed to traverse gap distances of up to 20 mm.

Stagnation particle velocity measurements: In both sets of experiments conducted at 9.1 km/s and 10.1 km/s, the measured peak particle velocity produced by the liquid-vapor states stagnating at the aluminum witness plate depends on the propagation distance (*i.e.*, on gap size). The change in peak witness-plate velocity u_{wp} with respect to gap size is a strong indication of the amount of vaporization that occurs in the zinc over the time duration of the experiment. Figure 6 shows the variation of u_{wp} , with respect to gap size. u_{wp} is normalized with respect to the tantalum impact velocity V , and zero-gap velocity U_{max} , respectively, where

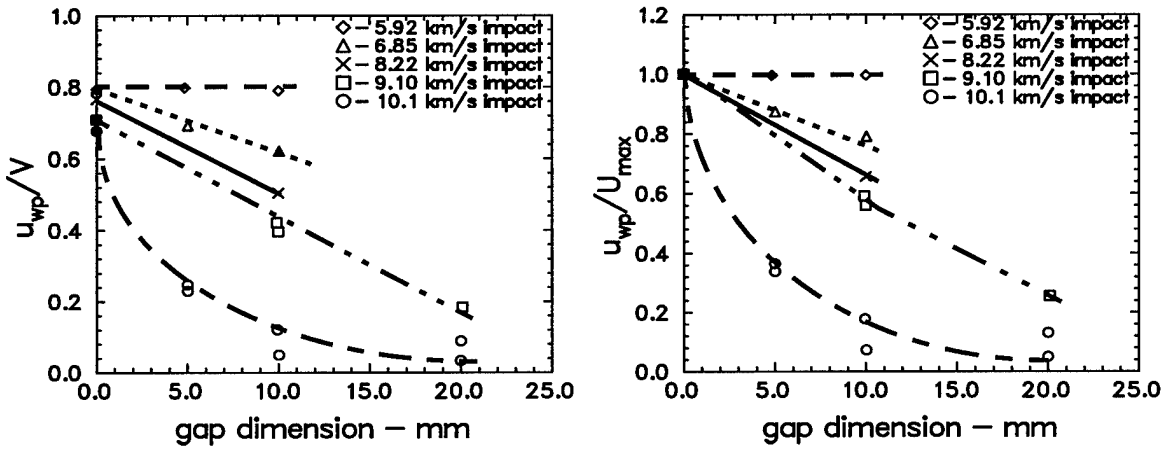


Figure 8. Normalized measured witness-plate peak velocity vs. propagation distance (i.e., gap size). The normalized factors are (a) tantalum impact velocity V and (b) the computed zero-gap peak velocity U_{max} (which depends on tantalum impact speed and experiment geometry).

U_{max} is the peak witness-plate velocity for a gap size of zero. The value of U_{max} is based on calculations.

The aluminum witness-plate/lithium-fluoride window can be regarded as a target with which the liquid/vapor debris cloud interacts. The peak interface velocity measurement u_{wp} is an indicator of the maximum stress resulting from this interaction. Observe that u_{wp}/V or u_{wp}/U_{max} are *higher* for the *lower*-speed 9.1 km/s shots than for the corresponding 10.1 km/s shots, which suggests that greater vaporization occurred in the 10.1 km/s shots. Figure 6, which summarizes all experimental data [17,23] shows that the peak witness-plate velocity u_{wp} and, therefore, the target/debris interaction stress, decrease monotonically with increasing propagation distance (gap size). All curves in Figure 8 must — in one-dimensional theory — asymptote to some constant value as gap size is increased. When such a curve asymptotes to zero, the sample must have vaporized completely. When a curve asymptotes to some non-zero value of u_{wp}/U_{max} , the sample must have only partially vaporized. When a curve is *constant*, no vaporization must have occurred and the maximum interaction stress must be independent of gap size. In Figure 8, the lowest speed experiment [23] (5.92 km/s) exhibits negligible expansion (i.e., the zinc target remains essentially intact as it crosses the gap). By contrast, the highest speed (10.1 km/s) experiment [17] shows considerable expansion of the zinc, which corresponds to a much lower stress on the buffer than the lower-speed lower-vaporization experiments. (Even though loading stress can be reduced substantially by vaporization, the survivability of any target nevertheless depends on many other parameters including the duration of the pressure pulse, the thickness of the target, and the yield and fracture strength of the target.) For zinc, the rapid approach to an asymptotic limit suggests that boiling occurs more rapidly from super-critical states.

Although not specifically discussed in this paper, the experiments have suggested a lack of agreement with CTH code calculations [24] using an existing ANEOS equation of state [25]. It should also be noted that the same ANEOS model, however, describes the impact experiments on zinc performed at lower impact velocities of 5.8 km/s to 7 km/s [23] quite satisfactorily. This clearly indicates a need to develop and/or refine current EOS models for zinc which describe the shock-induced vaporization process in extreme pressure and temperature regimes.

4. SUMMARY

Examples of experiments described in this report demonstrate the use of the hypervelocity launcher to determine material properties in pressure and temperature regimes that have never been accessible in the laboratory before. This has allowed the measurements of time-resolved wave profiles for shock loading and release experiments and stagnation pressure histories for zinc vaporization experiments. Only a brief summary is presented here to illustrate the use of HVL and time-resolved techniques for material properties measurements. The reader is encouraged to refer to the original articles for experimental details and experimental impact conditions. These experiments, due to their plate geometry, also serve to validate hydrodynamic codes in the impact regime (where very few experiments are available) not only for well-controlled EOS studies but also for ballistic applications [26-27].

It should be emphasized that most of the techniques used are those that were developed earlier for relatively lower impact studies. There is, however, a need for the development of techniques that would have better spatial resolution or time resolution that is commensurate with the physical processes that are being diagnosed. It is anticipated that successful experimental measurement of the material properties and the physical processes related to hypervelocity impact will eventually lead to the development and validation of constitutive and EOS models for material behavior that are needed for hydrodynamic code calculations for many programmatic needs related to hypervelocity impact [28-31] including ICF applications.

REFERENCES

1. J. R. Asay, L. C. Chhabildas and L. M. Barker, Sandia National Laboratories Report SAND85-2009, (1985) (unpublished).
2. A. C. Charters, Int., J. Impact Engng., V5 (1987) 181.
3. L. C. Chhabildas, in Recent Trend in High-Pressure Research, Proceedings of the XIII AIRAPT Conference on High Pressure Science and Technology, ed. by A. K. Singh, Bangalore, India, (1992) 739.
4. L. C. Chhabildas, Int., J. Impact Engng., V5 (1987) 205.
5. L. C. Chhabildas, and R. A. Graham, in AMD Vol. 83, ed., by R. Stout, F. Norwood, and M. Fournier, (1987) 1.
6. See for example LASL Shock Hugoniot Data, ed., by S. P. Marsh, University of California, Press, (1980).
7. J. R. Asay and L. C. Chhabildas, in Shock Waves and High-Strain-Rate Phenomena in Metals, Plenum Publishers, New York (1981).
8. J. R. Asay, L. C. Chhabildas, G. I. Kerley and T. G. Trucano, in *Shock Waves in Condensed Matter-1985*, ed. by Y. M. Gupta, Plenum Publishers, (1986) 145.
9. L. C. Chhabildas, L. M. Barker, J. R. Asay and T. G. Trucano, Int. J. Impact Engng., V10 (1990) 107.
10. L. C. Chhabildas and J. R. Asay in Shock Waves and High-Strain-Rate Phenomena in Materials, Marcel Decker, New York (1992) 947.
11. J. R. Asay, T. G. Trucano and L. C. Chhabildas, in *Shock Waves in Condensed Matter-1987*, ed. by S. C. Schmidt, J. W. Forbes and N. C. Holmes, Elsevier Science Publishers, (1988) 159.

12. J. R. Asay, T. G. Trucano and R. S. Hawke, *Int. J. Impact Engng.*, V10, (1990) 51.
13. J. R. Asay and G. I. Kerley, *J. Impact Engng.*, V5, (1987) 69.
14. L. C. Chhabildas, L. M. Barker, J. R. Asay, T. G. Trucano, G. I. Kerley and J. E. Dunn, in *Shock Waves in Condensed Matter-1991*, ed. by S. C. Schmidt, R. D. Dick, J. W. Forbes and D. G. Tasker, Elsevier Science Publishers, (1992) 1025.
15. L. C. Chhabildas, J. E. Dunn, W. D. Reinhart and J. M. Miller, *Int. J. Impact Engng.*, V14, (1993) 121.
16. L. C. Chhabildas, L. N. Kmetyk, W. D. Reinhart and C. A. Hall, *Int. J. Impact Engng.*, V17, (1995) 183.
17. R. M. Brannon and L. C. Chhabildas, *Int. J. Impact Engng.*, V17, (1995) 109.
18. L. M. Barker, in *Shock Waves in Condensed Matter-1983*, ed. by J. R. Asay, R. A. Graham, and G. K. Straub, Elsevier Science Publishers, (1984) 217.
19. J. L. Wise and L. C. Chhabildas, in *Shock Waves in Condensed Matter-1985*, ed. by Y. M. Gupta, Plenum Publishers, (1986) 441.
20. L. M. Barker and R. E. Hollenbach, *J. Appl. Phys.*, 43 (1972) 4669.
21. G. I. Kerley, *Int. J. Impact Engng.*, V5, (1987) 441.
22. R. G. McQueen, J. N. Fritz, and C. E. Morris, in *Shock Waves in Condensed Matter-1983*, ed. by J. R. Asay, R. A. Graham, and G. K. Straub, Elsevier Science Publishers, (1984) 95.
23. J. L. Wise, G. I. Kerley, T. G. Trucano, ed. by S. C. Schmidt, R. D. Dick, J. W. Forbes and D. G. Tasker, Elsevier Science Publishers, (1992) 61.
24. J. M. McGlaun, F. J. Zeigler, S. L. Thompson and M. G. Elrick, Sandia National Laboratories Report SAND88-0523, (1988).
25. S. L. Thompson, Sandia National Laboratories Report SAND89-2951, May (1990).
26. L. C. Chhabildas, W. D. Reinhart and C. A. Hall, Space Programs and Technologies Conference, AIAA Paper 94-4538 (1994).
27. L. C. Chhabildas Hypervelocity Impact Phenomena, *Published in the Metallurgical and Materials Applications of Shock-Wave and High-Strain-Rate Phenomena*, Elsevier Science Publishers, (1995) 245.
28. C. H. Konrad, L. C. Chhabildas, M. B. Boslough, A. J. Piekutowski, K. L. Poormon, S. A. Mullin and D. L. Littlefield, High-Pressure Science and Technology-1993, AIP Conference Proceedings 309, V2, (1994) 1845.
29. L. C. Chhabildas, E. S. Hertel, S. A. Hill, in *Proceedings of the Hypervelocity Impact Symposium-1991*, University of Kent at Canterbury, Kent, U.K., ed. by J. A. M. McDonnell (1992) 247.
30. M. B. Boslough, J. A. Ang, L. C. Chhabildas, B. G. Cour-Palais, E. C. Christiansen, J. L. Crews, W. D. Reinhart, and C. A. Hall, *Int. J. Impact Engng.*, V14, (1993) 95.
31. R. J. Lawrence, L. N. Kmetyk and L. C. Chhabildas, *Int. J. Impact Engng.*, V17, (1995).

M98004129



Report Number (14) SAND--97-3094C
CONF-980218--

Publ. Date (11) 199802

Sponsor Code (18) DOE/DP, XF

JC Category (19) KC-700, DOE/ER

DOE